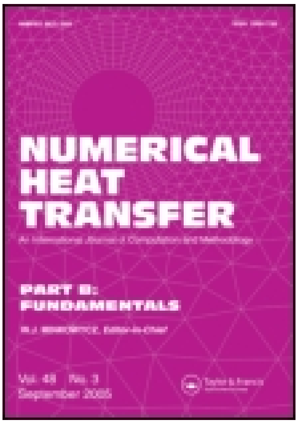

Numerical Heat Transfer, Part B: Fundamentals
Publication details, including instructions for authors and subscription information:
http://www.tandfonline.com/loi/unhb20

An Accurate Nodal Heat Balance Integral Method with Spatial Subdivision

S. L. Mitchell [a]
[a] Department of Mathematics and Statistics, MACSI, University of Limerick, Limerick, Ireland

Available online: 05 Jul 2011

To cite this article: S. L. Mitchell (2011): An Accurate Nodal Heat Balance Integral Method with Spatial Subdivision, Numerical Heat Transfer, Part B: Fundamentals, 60:1, 34-56

To link to this article: http://dx.doi.org/10.1080/10407790.2011.588133

Numerical Heat Transfer, Part B, 60: 34–56, 2011

ISSN: 1040-7790 print/1521-0626 online
DOI: 10.1080/10407790.2011.588133

AN ACCURATE NODAL HEAT BALANCE INTEGRAL METHOD WITH SPATIAL SUBDIVISION

S. L. Mitchell
Department of Mathematics and Statistics, MACSI, University of Limerick, Limerick, Ireland

This article presents a new form of the heat balance integral method in which the spatial variable is subdivided into equal intervals and an approximating profile is specified in each subdivision. Although the nodal refinement to the classic heat balance integral method is well documented, these studies have only been applied to classic thermal or Stefan problems with a fixed boundary condition prescribed at $x = 0$, and break down for more realistic boundary conditions such as constant flux, Newton cooling, or time-dependent conditions. There are also issues regarding how to start up the computation for a region which initially has zero thickness. Here we apply the so-called boundary immobilization technique, along with piecewise smooth approximating profiles, which eliminates the need for a separate starting procedure and gives far more accurate results. This is demonstrated for both thermal and Stefan problems and a variety of boundary conditions.

1. INTRODUCTION

The heat balance integral method (HBIM) is a well-known approximate technique for solving thermal problems. It was originally proposed by Goodman [11–13] as an adaptation of the Karman-Pohlhausen integral method [33] for analyzing boundary layers in fluid flow. It has made its greatest impact on Stefan problems, where very few exact solutions exist; see [20] and references therein. However, it has also been applied to many other applications, such as problems in viscous flow [25, 39], the Korteweg-de-Vries equation [29], microwave heating of grain [32], and rewetting of surfaces [37]. Other approximate solution techniques obviously exist, such as numerical methods, perturbation solutions, and ray methods; see, for example, [1, 6, 9, 14, 16, 19, 22, 30]. Despite the fact that the HBIM is generally not as accurate as these methods, it remains a popular choice due to its simplicity and the fact that it produces analytic solutions for a wide range of problems and parameter values.

However, the method has various well-known drawbacks, the most important being that the choice of approximating function is arbitrary, and this is key to the

Received 22 October 2010; accepted 29 April 2011.

The author acknowledges the support of the Mathematics Applications Consortium for Science and Industry (MACSI, www.macsi.ul.ie), funded by Science Foundation Ireland Mathematics Initiative Grant 06/MI/005.

Address correspondence to Sarah L. Mitchell, MACSI, Department of Mathematics and Statistics, University of Limerick, Limerick, Ireland. E-mail: sarah.mitchell@ul.ie

method's accuracy. To compound the ambiguity, there are often different ways to formulate even the most basic problem, see [20, 41], and this also affects the accuracy. Goodman's [11–13] original approach, applied to one-dimensional heat transfer problems both with and without a change of phase, was to define a single profile which would hold over the entire domain. He began with quadratic polynomial profiles but also discussed using cubic profiles, and this generally led to more accurate solutions [20].

Recently, Mitchell and Myers [21, 24, 26–28] have addressed the issue of the choice of approximating function and obtain significantly more accurate results than from using a polynomial profile. The exponent is not specified *a priori* or chosen by comparison with exact solutions or boundary conditions [5, 15]. Myers [24, 26] chose to determine the exponent from minimizing a least-squares error originally defined by Langford [17], and more recently adapted to avoid the singularity at $t = 0$ [28]. An alternative approach, developed by Mitchell and Myers [21, 27] combines the heat balance integral method with Sadoun's [35] refined integral method (RIM), and uses this extra equation to determine the exponent n. The minimization method is generally more accurate, but the combined integral method (CIM) is usually more straightforward to formulate and allows n to be time dependent, which is the case for certain boundary conditions [21].

This article aims to develop a general refined and highly accurate method which avoids the problem of how to choose the approximating function, though still utilizing the basic idea behind the HBIM. Since there is no agreed way to measure the accuracy, many authors limit their studies to test problems with exact solutions, and often require a special starting procedure to deal with a region which initially has zero thickness [3, 7]. We apply the so-called boundary immobilization technique, which eliminates the need for a separate starting procedure and naturally allows us to apply our method to both thermal and Stefan problems and a variety of boundary conditions. Instead of using a single profile defined over the entire domain, the spatial variable is subdivided into equal intervals and an approximating profile is specified in each subdivision.

Noble [31] first suggested ways to improve the heat balance integral method by incorporating it into a numerical approach. The spatial variable was subdivided, and low-order polynomial profiles were used in each subregion; this was explored by Bell [2, 3] for classic Stefan problems in both planar and cylindrical geometries. There the dependent temperature variable was subdivided equally, instead of the spatial variable, and a quadratic profile was assigned in each subdivision. The idea of subdividing the independent spatial variable was considered by Bell [4] for the problem without phase change, and more recently in [23, 40] for the problem with phase change. Both these works used linear profiles which converge to the exact solution. However, as pointed out, in [36], this requires an increase of subregions, causing the nodal HBIM to become a numerical procedure and thus losing its simplicity.

In this work we are able to use a small number of subregions while still giving an accurate solution, for problems both with and without a change of phase. As discussed above, there is a choice in whether to subdivide the dependent or independent variable, but we find that the latter is more convenient, as it leads to a simpler, and more natural, formulation. We also focus attention on smooth profiles, as considered in [2, 3, 4], rather than linear profiles [4, 7, 23, 36, 40]. For certain time dependent boundary conditions, linear profiles break down: For example, if a monotonically decreasing function is prescribed, the temperature profile has a turning point which cannot be accurately captured using a linear profile, even if a large number of subdivisions is used.

We also address the issue of how to initiate a computation for a region which initially has zero thickness. A common solution, see [2, 7] among others, is to use a small time series solution as introduced by Poots [34]. However, we consider a different approach, which eliminates the need for an *ad hoc* treatment of the starting solution, recently developed by Mitchell and Vynnycky [22] for the numerical solution of Stefan problems using finite-difference methods. After applying the boundary immobilization method [8, 10, 16, 38], the computational domain will initially be of finite nonzero thickness. The transformation makes it is easy to relate different boundary conditions in the limit as $t \to 0$, which is useful in that it gives initial conditions when the resulting system of equations are ordinary differential equations (ODEs) rather than algebraic equations. Previous studies all focus on the basic test problems with fixed temperature conditions applied at the left boundary, and their methods are not easily adapted to other, more realistic boundary conditions.

This article is organized as follows. Section 2 considers the basic thermal problem without a change of phase. We begin by giving an overview of Goodman's classic HBIM and recent developments by Mitchell and Myers [21, 24, 26–28]. Then we describe Bell's [4] refinement using equal spatial subdivisions combined with linear profiles. In Section 3 we adapt this approach by combining the boundary immobilization technique with smooth profiles and apply the new method to several standard boundary conditions. The extension to Stefan problems is discussed in Section 4, and then conclusions are drawn in Section 5.

2. THE THERMAL PROBLEM

Consider the problem of heating a semi-infinite solid by specifying a constant temperature at the boundary $x = 0$. In nondimensional form this may be specified as

$$\frac{\partial T}{\partial t} = \frac{\partial^2 T}{\partial x^2} \quad 0 < x < \infty \tag{1}$$

$$T = 0 \quad \text{at } t = 0 \tag{2}$$

$$T = 1 \quad \text{at } x = 0 \tag{3}$$

$$T \to 0 \quad \text{as } x \to \infty \tag{4}$$

The well-known exact solution is

$$T(x,t) = \operatorname{erfc}\left(\frac{x}{2\sqrt{t}}\right) \tag{5}$$

Bell and Abbas [4] describe Goodman's [11, 12] original heat balance integral method along with a refinement using spatial subdivision and piecewise linear profiles. In this work we improve their solution by using piecewise smooth profiles and a boundary immobilization technique, making the method applicable for more realistic boundary conditions. We also compare the results with those of Mitchell and Myers [21], who have greatly improved the accuracy of Goodman's method by determining the exponent of the polynomial profile as part of the solution process, and also by adapting the polynomial profile to include a logarithmic term.

2.1. The Classic HBIM

For the above initial-boundary-value problem Goodman's classic HBIM involves three steps:

1. First we define the heat penetration depth, $\delta(t)$. For $x \geq \delta$ the temperature change from the initial temperature is assumed to be negligible.
2. An approximating function, typically a polynomial, is then introduced. This describes the temperature for $0 \leq x \leq \delta(t)$.
3. Finally, the heat equation is integrated over $x \in [0, \delta]$ to produce the heat balance integral. This results in a single ordinary differential equation for δ, which may often be solved analytically.

Once δ has been determined, the temperature T is known from the approximating function which is given in terms of δ. An alternative approach, developed by Sadoun and Si-Ahmed [35], is the refined integral method (RIM), which simply involves carrying out a double integration of the heat equation at stage 3. The relative merits of the two approaches, as well as a number of variations involving alternative approximating function's are described in detail in [20].

The standard approximating polynomial for the HBIM has the form

$$T = \left(1 - \frac{x}{\delta}\right)^m \tag{6}$$

This satisfies the far-field condition $T_x(\delta, t) = 0$ provided $m > 1$. In addition, a further condition on the curvature is often applied. It is derived by noting that

$$\frac{DT}{Dt}(\delta, t) = \left(\frac{\partial T}{\partial t} + \frac{\partial T}{\partial x}\frac{d\delta}{dt}\right)\bigg|_{x=\delta} = 0 \Rightarrow \frac{\partial^2 T}{\partial x^2}(\delta, t) = 0 \tag{7}$$

If this condition is also imposed, then we require $m > 2$. In general, m is chosen arbitrarily, and usually to provide the simplest profile that satisfies the boundary conditions. Consequently, $m = 2$ or 3 are the most common choices. With m specified, the problem reduces to determining δ.

The HBIM involves integrating the heat equation (1) with respect to x over the domain $[0, \delta(t)]$ [noting that $T_x(\delta, t) = 0$], and taking the time derivative outside of the integral [noting that $T(\delta, t) = 0$],

$$\frac{d}{dt}\int_0^{\delta} T\, dx = -\frac{\partial T}{\partial x}\bigg|_{x=0} \tag{8}$$

The RIM is derived by integrating the heat equation twice with respect to x and then integrating the left-hand side by parts. This gives

$$\delta\int_0^{\delta}\frac{\partial T}{\partial t}dx-\int_0^{\delta}x\frac{\partial T}{\partial t}\,dx=-T|_{x=0}-\delta\frac{\partial T}{\partial x}\bigg|_{x=0}$$

However, since $T_t=T_{xx}$, the first term on the left-hand side can be integrated again, and we obtain

$$\frac{d}{dt}\int_0^{\delta}xT\,dx=T|_{x=0} \tag{9}$$

Substituting T from Eq. (6) into (8) and (9) gives the following expressions:

$$\text{HBIM: }\ \frac{d}{dt}\left(\frac{\delta}{m+1}\right)=\frac{m}{\delta}\quad\text{RIM: }\ \frac{d}{dt}\left[\frac{\delta^2}{(m+1)(m+2)}\right]=1 \tag{10}$$

Assuming that m is constant, in both cases integration subject to $\delta(0)=0$ leads to $\delta=\alpha\sqrt{t}$, where

$$\text{HBIM:}\quad \alpha=\sqrt{2m(m+1)}\quad\text{RIM:}\quad \alpha=\sqrt{(m+1)(m+2)} \tag{11}$$

The method in [21], which is called the combined integral method (CIM), requires that δ is equal for either the HBIM or RIM. In this case we simply equate the expressions for α in (11) to find $m=2$. We note here that the minimization technique of Myers [24], which involves choosing m from minimizing $E=\int_0^{\delta}[T_t-T_{xx}]^2\,dx$, predicts $m=2.2335$ and 2.2185 for the HBIM and RIM, respectively. These refinements to obtain a more accurate value of m take away some of the arbitrary nature of the heat balance integral method. However, as we will show in the results below, assigning a single profile to the temperature can lead to very inaccurate results, and even break down completely, for certain boundary conditions.

An alternative to the polynomial profile (6) was developed by Mitchell and Myers [21], and is discussed in more detail in Appendix A.

2.2. A Simple Refinement Using Spatial Subdivision

Bell and Abbas [4] suggested a refinement to Goodman's method which incorporates the heat balance integral into a numerical approach. This involves subdividing the penetration depth $\delta(t)$ equally and solving for the values of T in each subdivision.

Suppose that $x\in[0,\delta]$ is subdivided into n equal subintervals of length δ/n (see Figure 1), where

$$T(x_i,t)=T_i\quad x_i=\frac{i\delta}{n}\quad i=0,1,\ldots,n \tag{12}$$

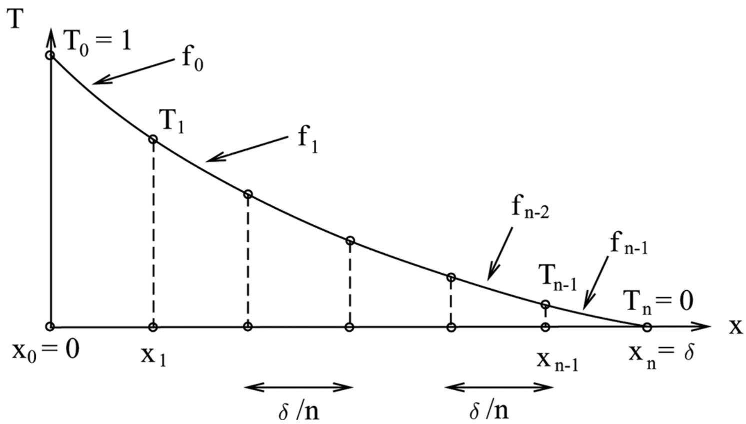

Figure 1. Equal subdivision of the region $0 < x < \delta$.

and the boundary conditions give $T_0 = 1$ and $T_n = 0$. The heat balance integral is now determined over each subinterval $[x_i, x_{i+1}]$, and so (8) becomes

$$\frac{d}{dt}\int_{x_i}^{x_{i+1}} T\,dx - x'_{i+1}T_{i+1} + x'_i T_i = \left.\frac{\partial T}{\partial x}\right|_{x=x_{i+1}} - \left.\frac{\partial T}{\partial x}\right|_{x=x_i} \tag{13}$$

for $i = 0, 1, \ldots, n-1$, or, in view of the definition of x_i in (12), this can be written as

$$\frac{d}{dt}\left[\int_{x_i}^{x_{i+1}} T\ dx - \frac{(i+1)T_{i+1}\delta}{n} + \frac{iT_i\delta}{n}\right] = \left.\frac{\partial T}{\partial x}\right|_{x=x_{i+1}} - \left.\frac{\partial T}{\partial x}\right|_{x=x_i} \tag{14}$$

for $i = 0, 1, \ldots, n-1$. Bell and Abbas [4] choose to approximate the temperature T in each subinterval $[x_i, x_{i+1}]$ by n piecewise linear profiles of the form

$$f_i(x) = T_i + (T_{i+1} - T_i)\frac{x - x_i}{x_{i+1} - x_i} \quad i = 0,\ 1, \ldots, n-1 \tag{15}$$

which automatically satisfy $f_i(x_i) = T_i$ and $f_i(x_{i+1}) = T_{i+1}$. Replacing T with f_i in (14) leads to

$$-\frac{(2i+1)(T_{i+1} + T_i)}{2n}\delta_t = f'_i(x_{i+1}) - f'_i(x_i) \tag{16}$$

Since we are using linear profiles, the derivative $f'_i(x)$ is constant, so direct substitution of (16) would give zero right-hand side. To avoid this problem [4], represent the change in flux by the discontinuous change in adjacent profile gradients, i.e., by setting

$$f'_i(x_i) = \frac{T_{i+1} - T_i}{x_{i+1} - x_i} = \frac{T_{i+1} - T_i}{\delta/n} \quad i = 0,\ 1, \ldots, n-1 \tag{17}$$

with $f_n'(x_{n+1}) = 0$ [since $T_x(\delta, t) = 0$]. We therefore obtain equations

$$\delta\delta_t = -\frac{2n^2}{2i+1}\frac{T_{i+2} - 2T_{i+1} + T_i}{T_{i+1} - T_i} \quad i = 0,\ 1, \ldots,\ n-2 \tag{18}$$

together with

$$\delta\delta_t = -\frac{2n^2}{2n-1} \tag{19}$$

which comes from the last subinterval, $i = n - 1$. Then δ is immediately determined as

$$\delta = \sqrt{\frac{4n_2\, t}{2n-1}} \tag{20}$$

and combining (18) and (19) eliminates the $\delta\delta_t$ term, resulting in the expression

$$(2n-1)T_{i+2} - (4n-2i-3)T_{i+1} + (2n-2i-2)T_i = 0 \tag{21}$$

for $i = 0, 1, \ldots, n-2$. This gives a system of $n-1$ linear equations for the unknowns T_1, $T_2, \ldots, T_{n-1}$. An exact expression for the T_i's can be determined by back substitution:

$$T_i = T_{n-1}\sum_{j=1}^{n-1}\frac{\left(n-\frac{1}{2}\right)^{j-1}}{(j-1)!} \quad i = 0,\ 1, \ldots,\ n-2 \tag{22}$$

Setting $i = 0$ gives T_{n-1} (since $T_0 = 1$), and we find

$$T_i = \frac{\sum_{j=1}^{n-i}\left[\left(n-\frac{1}{2}\right)^{j-1}/(j-1)!\right]}{\sum_{j=1}^{n}\left[\left(n-\frac{1}{2}\right)^{j-1}/(j-1)!\right]} \tag{23}$$

The approximate solution (15) can be shown to converge to the exact solution (5) as $n \to \infty$ [4]. However, from a computational point of view, we would like to obtain an accurate solution using a small value of n. It is also clear that this profile is not very accurate for small n, because the linear profile cannot match derivatives at each node point x_i.

3. A SMOOTH PROFILE USING AN IMMOBILIZED BOUNDARY

One obvious way to improve the Bell and Abbas technique would be to include higher-order terms in (15) and then match the appropriate number of derivatives to determine the extra unknown coefficients. This is straightforward for the classic problem (1)–(4), and results using quadratic and cubic profiles give a significant improvement to the linear profile. These also avoid the problem of having zero right-hand side in (14). However, since the T_i's are assumed here to be constant, this method cannot be applied to other types of boundary conditions, such as constant flux or cooling conditions. For example, in place of (15), a quadratic profile would be of the form

$$f_i(x) = T_i + \frac{\alpha(x - x_i)}{x_{i+1} - x_i} + \frac{\beta_i(x - x_i)^2}{(x_{i+1} - x_i)^2} \quad i = 0,\ 1, \ldots, n-1 \tag{24}$$

where the coefficients α_i and β_i come from requiring $f_i(x_{i+1}) = T_{i+1}$ and $f_i'(x_{i+1}) = f_{i+1}'(x_{i+1})$. If the boundary condition at $x = 0$ is the constant flux condition $T_x = -1$, then this means that $f_0'(x_0) = -1$. Using (24) and the definition of x_i in (12), it follows that $\alpha_0 = -\delta/n$. Thus α_0 is time dependent, which cannot be dealt with using the Bell and Abbas method.

We therefore now describe an alternative approach which is far more general and can easily be adapted to other boundary conditions, including time-dependent conditions. It involves immobilizing the boundary and therefore converts the moving domain $0 < x < \delta(t)$ into one which is fixed for all time. For convenience we restate the problem as

$$\frac{\partial T}{\partial t} = \frac{\partial^2 T}{\partial x^2} \quad 0 < x < \delta(t) \tag{25}$$

$$T = 0 \quad \text{at } t = 0 \tag{26}$$

$$T = \frac{\partial T}{\partial x} = 0 \quad \text{at } x = \delta \tag{27}$$

with the following boundary conditions at $x = 0$:

$$\text{(i)} \quad T = 1 \quad \text{(ii)} \quad \frac{\partial T}{\partial x} = -1 \quad \text{(iii)} \quad \frac{\partial T}{\partial x} = T - 1 \quad \text{(iv)} \quad T = h(t) \tag{28}$$

Boundary conditions (ii) and (iii) are the constant flux and cooling conditions, respectively, and in (iv) we assume without loss of generality that $h(0) = 1$.

Since the penetration depth δ is initially of zero thickness, it is advantageous to work in transformed coordinates by introducing a boundary immobilization technique. For the most general case, we set

$$\xi = \frac{x}{\delta(t)} \quad T(x, t) = \phi(t) F(\xi, t) \tag{29}$$

so that Eqs. (25), (27), and (28) become

$$\phi \frac{\partial^2 F}{\partial \xi^2} = \delta\left(\delta \phi_t F + \delta \phi \frac{\partial F}{\partial t} - \xi \delta_t \phi \frac{\partial F}{\partial \xi}\right) \tag{30}$$

$$F = \frac{\partial F}{\partial \xi} = 0 \quad \text{at } \xi = 1 \tag{31}$$

$$\text{(i)}\quad F=\frac{1}{\phi}\quad \text{(ii)}\quad \frac{\partial F}{\partial \xi}=-\frac{\delta}{\phi}\quad \text{(iii)}\quad \frac{\partial F}{\partial \xi}=\delta\left(F-\frac{1}{\phi}\right)$$
$$\text{(iv)}\quad F=\frac{h}{\phi}\quad \text{at}\quad \xi=0 \tag{32}$$

Following Mitchell and Vynnycky [22], we choose $\phi(t)$ in such a way as to ensure that a self-consistent boundary-value problem is obtained in the limit as $t\to 0$, in the sense that the solution of the resulting ODE in this limit is consistent with the solution of the PDE for arbitrary time.

i. For boundary condition (32i), the choice $\phi(t)=1$ ensures that $F(0, t)=1$, which is independent of time as $t\to 0$. Then (30) reduces to

$$\frac{\partial^2 F}{\partial \xi^2}=\delta^2\frac{\partial F}{\partial t}-\xi\delta\delta_t\frac{\partial F}{\partial \xi} \tag{33}$$

ii. In the case of boundary condition (32ii), it is clear that we must now choose $\phi(t)=\delta(t)$, giving $F_\xi(0, t)=-1$. Now (30) becomes

$$\frac{\partial^2 F}{\partial \xi^2}=\delta\delta_t F+\delta^2\frac{\partial F}{\partial t}-\xi\delta\delta_t\frac{\partial F}{\partial \xi} \tag{34}$$

iii. For boundary condition (32iii), it also follows that $\phi(t)=\delta(t)$, and so the PDE (30) is again given by (34) with $F_\xi(0, t)=\delta F(0, t)-1$.

iv. Finally, for the time-dependent boundary condition (32iv), the choice $\phi(t)=h(t)$ ensures that $F(0, t)=1$, which is independent of time as $t\to 0$. Here (30) is now

$$h\frac{\partial^2 F}{\partial \xi^2}=\delta^2 h_t F+\delta^2 h\frac{\partial F}{\partial t}-\xi\delta\delta_t h\frac{\partial F}{\partial \xi} \tag{35}$$

3.1. Boundary Condition (I)

After the transformation given in (29), we can see from (6) that the standard polynomial profile used in the HBIM is now simply $F=(1-\xi)^n$. This profile is independent of δ, and therefore t, which suggests we look for a time-independent spline profile.

We now apply the nodal heat balance integral method to this transformed problem. Another advantage of the transformation (29) is that the domain ξ is fixed, and so we can subdivide ξ equally and these are now independent of δ. Hence we set

$$F(\xi_i)=F_i\quad \xi_i=\frac{i}{n}\quad i=0,\ 1,\ \ldots,\ n \tag{36}$$

and the boundary conditions become $F_0 = 1$, $F_n = 0$. In place of (13), the heat balance integral is now

$$-\delta\delta_t\left(\xi_{i+1}F_{i+1} - \xi_i F_i - \int_{\xi}^{\xi_{i+1}} F d\xi\right) = \left.\frac{\partial F}{\partial \xi}\right|_{\xi=\xi_{i+1}} - \left.\frac{\partial F}{\partial \xi}\right|_{\xi=\xi_i} \tag{37}$$

for $i = 0, 1, \ldots, n-1$. As mentioned above, the simplest refinement to obtain a piecewise smooth profile in each subinterval is to use a quadratic profile with the first derivatives being matched at each nodal point. However, this is essentially a spline interpolation; and quadratic splines are well known for giving severe oscillation effects. We therefore give details for a cubic profile, as this is a much more popular choice in the field of spline interpolation; the analysis for the quadratic profile is given in Appendix B. Since the cubic profile requires matching the first and second derivatives at each nodal point, it involves slightly more work than for the quadratic profile, but it ensures a smooth profile for the derivative of the temperature, as well as the temperature itself.

At each subinterval $[\xi_i, \xi_{i+1}]$, F is a approximated by the following cubic profile:

$$f_i(\xi) = F_i + \frac{\alpha_i(\xi - \xi_i)}{\xi_{i+1} - \xi_i} + \frac{\beta_i(\xi - \xi_i)^2}{(\xi_{i+1} - \xi_i)^2} + \frac{\gamma_i(\xi - \xi_i)^3}{(\xi_{i+1} - \xi_i)^3} \tag{38}$$

for $i = 0, 1, \ldots, n-1$, with the coefficients α_i, β_i, and γ_i being determined as part of the solution process by matching the f_i's and their first and second derivatives at each nodal point. Note that, written in this form we already have $f_i(\xi_i) = F_i$, and so to ensure $f_i(\xi_{i+1}) = F_{i+1}$ we must satisfy

$$\alpha_i + \beta_i + \gamma_i = F_{i+1} - F_i \quad i = 0, 1, \ldots, n-1 \tag{39}$$

Matching first and second derivatives, i.e., $f_i'(\xi_{i+1}) = f_{i+1}'(\xi_{i+1})$ and $f_i''(\xi_{i+1}) = f_{i+1}''(\xi_{i+1})$, gives

$$\alpha_i + 2\beta_i + 3\gamma_i = \alpha_{i+1} \quad 2\beta_i + 6\gamma_i = 2\beta_{i+1} \quad i = 0, 1, \ldots, n-2 \tag{40}$$

Since $F_\xi(1, t) = 0$, it follows that $f_{n-1}'(\xi_n) = 0$. With the added assumption that $F_{\xi\xi}(1, t) = 0$, which is reasonable in view of (7), we can also set $f_{n-1}''(\xi_n) = 0$. This leads to

$$\alpha_{n-1} + 2\beta_{n-1} + 3\gamma_{n-1} = 0 \quad 2\beta_{n-1} + 6\gamma_{n-1} = 0$$

Combining these expressions with the $i = n-1$ equation in (39), using the fact that $F_n = 0$, we obtain

$$\alpha_{n-1} = -3F_{n-1} \quad \beta_{n-1} = 3F_{n-1} \quad \gamma_{n-1} = -F_{n-1} \tag{41}$$

Substituting the cubic profile (38) into the heat balance integral (37), we find [noting that we can use $f_i'(\xi)$ directly to calculate the derivatives on the right-hand side]

$$\delta\delta_t = \frac{n^2(2\beta_i + 3\gamma_i)}{\alpha_i/2 + \beta_i/3 + \gamma_i/4 - (i+1)(F_{i+1} - F_i)} \quad i = 0, 1, \ldots, n-1 \tag{42}$$

Setting $i=n-1$ and using the expressions in (41) leads to

$$\delta\delta_t = \frac{12n^2}{4n-3} \tag{43}$$

We now use this to eliminate $\delta\delta_t$ from (42) to give

$$3\alpha_i + (5-4n)\beta_i + 6(1-n)\gamma_i - 6(i+1)(F_{i+1} - F_i) = 0 \tag{44}$$

for $i=0, 1, \ldots, n-2$. Combining (39), (40), and (44) allows us to determine the $4n-1$ unknowns: α_i, β_i, γ_i for $i=0, 1, \ldots, n-1$ and F_i for $i=1, 2, \ldots, n-1$ [noting that δ is now known from (43)]. This can be achieved from writing the equations as the matrix system $A\mathrm{x}=\mathrm{b}$, where

$$\mathrm{x} = [F_0,\ \alpha_0,\ \beta_0,\ \gamma_0,\ F_1,\ \alpha_1,\ \beta_1,\ \gamma_1, \ldots, F_{n-1},\ \alpha_{n-1},\ \beta_{n-1},\ \gamma_{n-1}]^T \tag{45}$$

the matrix A contains (39), (40), (44), and the vector b has first entry equal to 1 and zeros elsewhere (to give the boundary condition $F_0=1$).

3.2. Boundary Condition (II)

The constant-flux boundary condition is very similar to the fixed boundary condition (i). In original variables, the standard heat balance polynomial is $T=(\delta/n)(1-x/\delta)^n$, and so after the transformation in (29) with $\phi=\delta$, we have $F=(1/n)(1-\xi)^n$. Again this is time independent, and so we make the additional assumption that the spline solution is also time independent; then we can set $F_t=0$ in (34). Here the heat balance integral is

$$-\delta\delta_t\left(\xi_{i+1}F_{i+1} - \xi_i F_i - 2\int_{\xi_i}^{\xi_{i+1}} F d\xi\right) = \left.\frac{\partial F}{\partial \xi}\right|_{\xi=\xi_{i+1}} - \left.\frac{\partial F}{\partial \xi}\right|_{\xi=\xi_i} \tag{46}$$

for $i=0, 1, \ldots, n-1$, and after substituting in the cubic profile (38) we obtain

$$\delta\delta_t = \frac{n^2(2\beta_i + 3\gamma_i)}{\alpha_i + 2\beta_i/3 + \gamma_i/2 - (i+1)F_{i+1} + (i+2)F_i} \tag{47}$$

Setting $i=n$ and using the expressions in (41) leads to

$$\delta\delta_t = \frac{6n^2}{2n-1} \tag{48}$$

We then substitute $\delta\delta_t$ into (47) to give

$$3\alpha_i + (3-2n)\beta_i + 3(1-n)\gamma_i - 3(i+1)F_{i+1} + 3(i+2)F_i = 0 \tag{49}$$

which is again combined with (39) and (40) to determine the unknown coefficients. The boundary condition $F_\xi=-1$ implies that $f_0'(\xi_0)=-1$, and this reduces to $\alpha_0=-1/n$.

The calculations for the quadratic profile are similar to boundary condition (i); see Appendix B.

3.3. Boundary Condition (III)

We now turn attention to the cooling condition (32iii). Here the standard heat balance polynomial is $T=[\delta/(n+\delta)](1-x/\delta)^n$, and so after the transformation in (29), again with $\phi=\delta$, the profile is given by the time-dependent expression $F=[1/(n+\delta)](1-\xi)^n$. This suggests that the unknowns α_i, β_i, γ_i, and F_i are not constant in time. Upon integrating (34) over the interval $[\xi_i, \xi_{i+1}]$, the heat balance integral becomes

$$-\delta\delta_t\left(\xi_{i+1}F_{i+1}-\xi_iF_i-2\int_{\xi_i}^{\xi_{i+1}}Fd\xi\right)+\delta^2\frac{d}{dt}\int_{\xi_i}^{\xi_{i+1}}Fd\xi=\left.\frac{\partial F}{\partial\xi}\right|_{\xi=\xi_{i+1}}-\left.\frac{\partial F}{\partial\xi}\right|_{\xi=\xi_i} \tag{50}$$

and after substituting in the cubic profile (38) we obtain

$$\begin{aligned}\left[\alpha_i+\frac{2\beta_i}{3}+\frac{\gamma_i}{2}-(i+1)F_{i+1}+(i+2)F_i\right]\delta\delta_t+\delta^2\frac{d}{dt}\\ \left(\frac{\alpha_i}{2}+\frac{\beta_i}{3}+\frac{\gamma_i}{4}+F_i\right)=n^2(2\beta_i+3\gamma_i)\end{aligned} \tag{51}$$

The boundary condition $F_\xi=-1$ implies that $f_0'(\xi_0)=\delta f_0(\xi_0)-1$, and this reduces to

$$n\alpha_0=\delta F_0-1 \tag{52}$$

The equations in (51) give a system of n ODEs, although in fact we need $4n$ equations in total to determine all the unknowns. The other ODEs are found from differentiating (39) and (40) with respect to t. The matrix system is then written as $Ax_t=b$, where x is defined in (45) but with δ as an extra entry. Also, the boundary condition (52) is differentiated with respect to t to give the final equation. In the limit as $t\to 0$, the equations for the cooling condition reduce to those for the constant-flux condition (ii). Therefore the initial conditions for x are just the values found for case (ii), along with $\delta(0)=0$. The resulting ODEs are solved using an ODE solver such as "ode45" in Matlab.

3.4. Boundary Condition (IV)

For the time-dependent boundary condition (iv), we must also solve a system of ODEs. After integrating (35) with respect to ξ from ξ_i to ξ_{i+1}, and substituting in the cubic profile (38), we find

$$\begin{aligned}&h\left[\frac{\alpha_i}{2}+\frac{\beta_i}{3}+\frac{\gamma_i}{4}-(i+1)(F_{i+1}-F_i)\right]\delta\delta_t+\delta^2h\frac{d}{dt}\left(\frac{\alpha_i}{2}+\frac{\beta_i}{3}+\frac{\gamma_i}{4}+F_i\right)\\ &=n^2(2\beta_i+3\gamma_i)-\delta^2h_t\left(\frac{\alpha_i}{2}+\frac{\beta_i}{3}+\frac{\gamma_i}{4}+F_i\right)\end{aligned} \tag{53}$$

This is very similar to boundary condition (iii), and so we solve $Ax_t = b$, where A consists of the equations in (53) along with (39), (40), and the boundary condition $F_1 = h$ (after differentiating them all with respect to t). Since $h(0) = 1$, the equations for this boundary condition reduce to those for the constant-temperature condition (i) in the limit as $t \to 0$; thus we use these coefficients as the initial conditions in x.

3.5. Results

In Figures 2 and 3 we compare results for the nodal HBIM described above (using linear, quadratic, and cubic profiles and $n = 4$ spatial subdivisions) with the CIM, as discussed in section 2.1. Figure 2 shows plots of the temperature profiles against x at fixed values of t. For boundary conditions (i)–(iii) we show only the nodal linear and cubic profiles, as it is hard to distinguish the quadratic from the cubic. The CIM solutions for these boundary conditions come from [21]: (i) uses (6) with $m = 2$, (ii) uses $T = (\delta/n)(1 - x/\delta)^m$ with $m = 4$, and (iii) uses $T = [\delta/(n + \delta)](1 - x/\delta)^m$ with $m = 3.585$. For the time-dependent boundary condition (iv), we consider the monotonically decreasing function $h(t) = 1 - t$, as this highlights

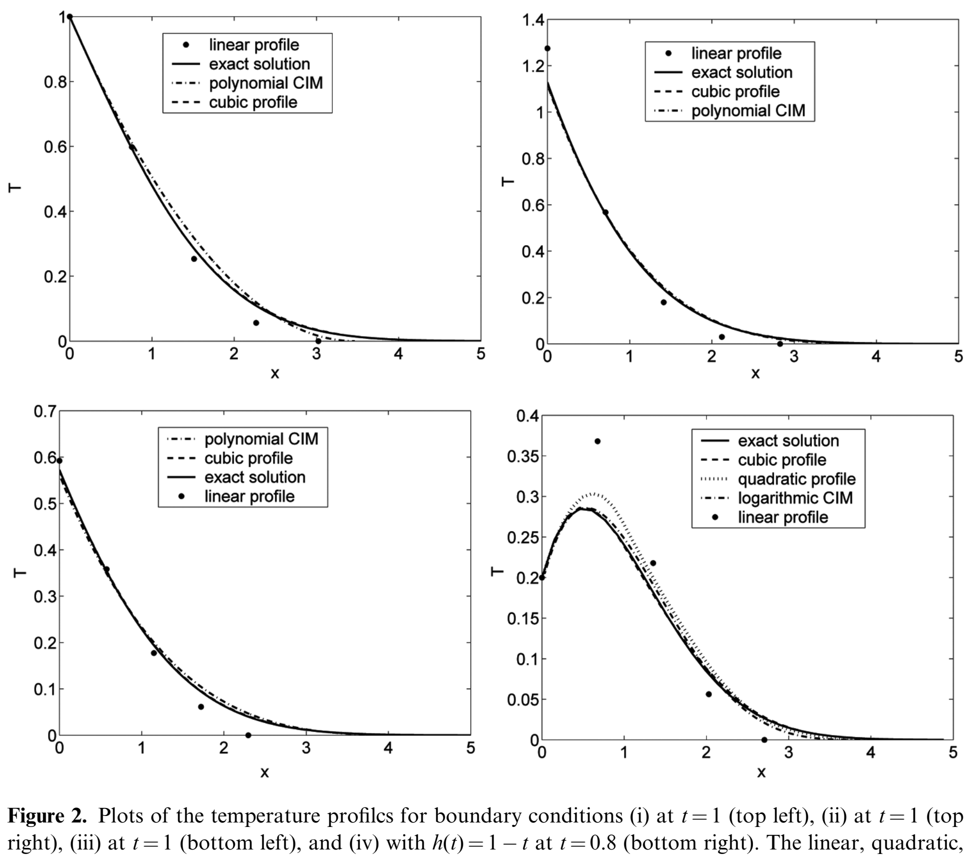

Figure 2. Plots of the temperature profiles for boundary conditions (i) at $t = 1$ (top left), (ii) at $t = 1$ (top right), (iii) at $t = 1$ (bottom left), and (iv) with $h(t) = 1 - t$ at $t = 0.8$ (bottom right). The linear, quadratic, and cubic profiles use $n = 4$.

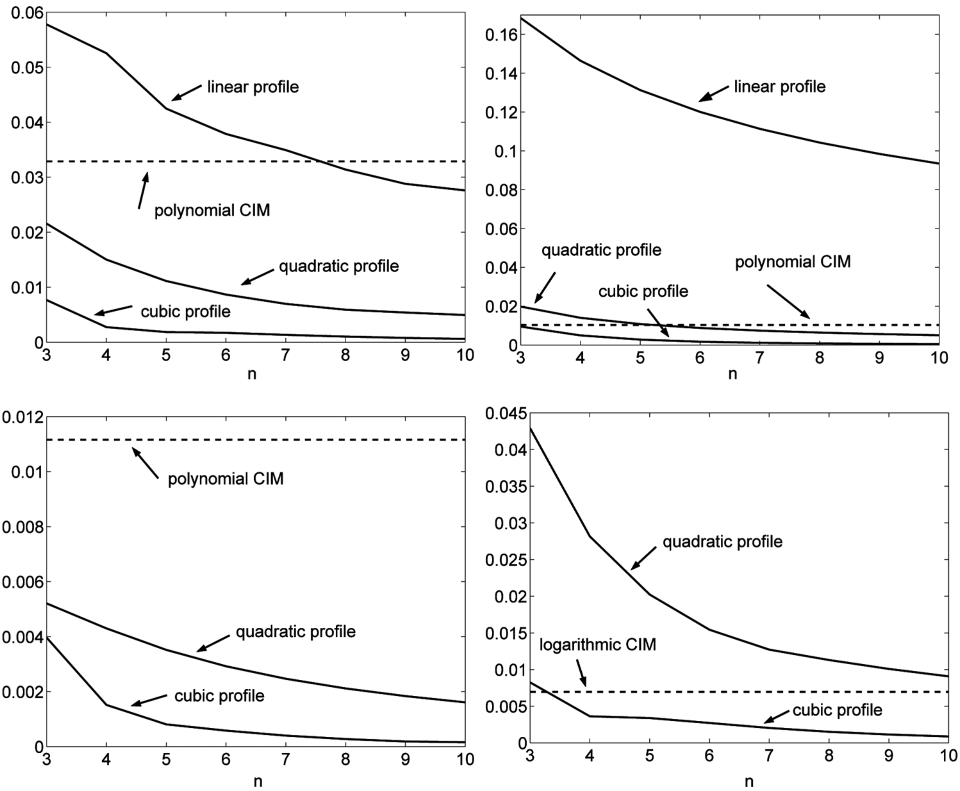

Figure 3. Maximum error versus n for boundary conditions (i) at $t = 1$ (top left), (ii) at $t = 1$ (bottom right), (iii) at $t = 1$ (bottom left), and (iv) with $h(t) = 1 - t$ at $t = 0.8$ (bottom right). The linear, quadratic, and cubic profiles use $n = 4$.

the weakness of polynomial profiles: They decrease monotonically from $x = 0$ to $x = \delta$ and so cannot capture the peak correctly. Instead, we have plotted the CIM with the logarithmic profile (66) and $m = 4.576$, as this allows a turning point in the temperature profile. Also note for boundary condition (iv) that the linear profile is very inaccurate and it is clear that a smooth profile is required. We have also shown the quadratic profile, since there is a noticeable difference between it and the cubic profile for this value of n. This example highlights the fact that the cubic profile performs much better when using a small number of subdivisions.

Figure 3 shows the maximum error in T against n for the linear, quadratic, and cubic profiles, at the same fixed values of t as in Figure 2. We have left off the linear profile in the bottom two plots, as it is much larger than the errors shown and its inclusion makes the other results hard to distinguish. For boundary condition (i) the polynomial CIM is always worse than the cubic or quadratic profiles, and better than the linear profile provided $n < 8$. For the constant-flux boundary condition (ii), the quadratic profile becomes more accurate than the polynomial CIM when $n > 5$, and for the cooling condition (iii) we see that the polynomial CIM is always worse than both the quadratic and cubic profiles (although more accurate than the linear profile for the values of n shown). The final plot in Figure 3 shows the time-dependent boundary condition (iv), and we see that the logarithmic profile does perform well compared with the quadratic profile but is still worse than the cubic profile.

4. THE STEFAN PROBLEM

The extension to Stefan problems turns out to be surprisingly straightforward. In nondimensional form the problem is described by

$$\frac{\partial T}{\partial t} = \frac{\partial^2 T}{\partial x^2} \quad 0 < x < s(t) \tag{54}$$

$$T = 0 \quad s = 0 \quad \text{at } t = 0 \tag{55}$$

$$T = h(t) \quad \text{at } x = 0 \tag{56}$$

$$T = 0 \quad \beta s_t = -\frac{\partial T}{\partial x} \quad \text{at } x = s \tag{57}$$

This is scaled in such a way that the parameter is the Stefan number $\beta = L_m/c_p\, \Delta T$, where L_m is the latent heat of melting, c_p is the specific heat capacity, and ΔT is the temperature variation. Again without loss of generality we assume that $h(0) = 1$. We have chosen a time-dependent boundary condition (56) to demonstrate the effectiveness of the new method: As for the thermal problem, traditional heat balance integral methods for Stefan problems break down for certain forms of $h(t)$, for example, periodic boundary conditions [35]. Other boundary conditions, such as a constant flux or cooling condition at $x = 0$, can also easily be handled by this method, but for brevity we do not include them here.

To immobilize the boundary we set

$$\xi = \frac{x}{s(t)} \quad T(x, t) = h(t)F(\xi, t) \tag{58}$$

and so (54) transforms into (35) but with δ replaced by s. The boundary conditions in (56) and (57) are now $F(0, t) = 1$ and $F(1, t) = 0$; the Stefan condition in (57) becomes

$$\beta s s_t = -h \frac{\partial F}{\partial \xi}\bigg|_{\xi=1} \tag{59}$$

Consider the same cubic profile as in (38), again with conditions (39) and (40) so that $f_i(x_{i+1}) = F_{i+1}$ and the first and second derivatives are matched at each nodal point. Then the heat balance integral leads to the system (53) but with $\delta = s$.

For the thermal problem we obtained two more equations from requiring $F_\xi(1, t) = F_{\xi\xi}(1, t) = 0$. These two conditions do not apply here, but we can instead use the Stefan condition (59) to deduce

$$\beta s s_t = -nh(\alpha_{n-1} + 2\beta_{n-1} + 3\gamma_{n-1}) \tag{60}$$

There is a choice in how to specify the final condition. A natural cubic spline formulation would set the second derivative to zero at the left boundary, i.e., $\beta_0 = 0$. However, to be more consistent with the thermal problem, we obtain an extra condition at the right boundary (which was first used by Goodman [11]). Similar to condition (7), in original variables we can take the total time derivative of $T(s, t) = 0$ to give

$$\frac{DT}{Dt}(s,t) = \left(\frac{\partial T}{\partial t} + \frac{\partial T}{\partial x}\frac{\mathrm{d}s}{\mathrm{d}t}\right)\bigg|_{x=s} = 0 \Rightarrow \beta\frac{\partial^2 T}{\partial x^2} = \left(\frac{\partial T}{\partial x}\right)^2\bigg|_{x=s} \tag{61}$$

After the transformation (58) this becomes

$$\beta\frac{\partial^2 F}{\partial \xi^2} = h\left(\frac{\partial F}{\partial \xi}\right)^2\bigg|_{\xi=1} \tag{62}$$

leading to the expression

$$\beta(2\beta_{n-1} + 6\gamma_{n-1}) = h(\alpha_{n-1} + 2\beta_{n-1} + 3\gamma_{n-1})^2 \tag{63}$$

4.1. The Classic Problem with $h(t) = 1$

The exact solution to (54)–(57) when $h = 1$ is given by the error-function solution

$$T(x,t) = 1 - \frac{\mathrm{erf}[x/(2\sqrt{t})]}{\mathrm{erf}(\alpha)} \quad s(t) = 2\alpha\sqrt{t} \tag{64}$$

where α satisfies the transcendental equation $\sqrt{\pi}\beta\alpha\,\mathrm{erf}(\alpha)e^{\alpha^2} = 1$. This problem is therefore very similar to the thermal problem with boundary condition (i) and so the coefficients α_i, β_i, γ_i, and T_i are constant in time. The heat balance integral is identical to (42) but with δ replaced by s. Previously, we could obtain expressions for α_{n-1}, β_{n-1}, and γ_{n-1} in terms of F_{n-1}, and combining with the $i = n - 1$ equation in (42), this led to the explicit expression (43) for $\delta\delta_t$ in terms of n only. Then $\delta\delta_t$ was eliminated from (42), which reduced to a linear set of equations. Although we can use (60) to eliminate ss_t in (42), this unfortunately does not give a linear system in the same way. However, the nonlinear set of equations can easily be solved using the Newton-Raphson method or a nonlinear solver package such as "fsolve" in Matlab.

Before presenting the results for this boundary condition, we first give the classic polynomial HBIM profile for the Stefan problem (54)–(57), which must be expressed in terms of the melt front s. We are unable to use a single-term model of the form (6) since, for $m > 1$, this gives $T_x(s, t) = 0$ and the melt front is stationary, while for $m < 1$ the front velocity is infinite. Consequently, we augment the expression with the simplest usable function, namely, a linear function

$$T = a\left(1 - \frac{x}{s}\right) + (h - a)\left(1 - \frac{x}{s}\right)^m \tag{65}$$

This form satisfies $T(0, t) = h(t)$ and $T(s, t) = 0$. At $x = s$, the gradient is $T_x(s, t) = -a/s$, so for a positive front velocity we require $a > 0$. The CIM then integrates the heat equation (54) over $x \in [0, s]$, either once or twice to obtain the HBIM and RIM formulations. Combining these with the Stefan condition in (57) then leads to three ODEs to solve for a, s, m.

Table 1 gives results for the classic Stefan problem with $h(t) = 1$. Both the percent error in α and the maximum error for the temperature T at a fixed time are shown. We have used $n = 4$ spatial subdivisions for the quadratic and cubic profiles. Notice that the CIM is only more accurate than the quadratic profile when $\beta = 10$, and this is only for the percent error in α. Otherwise, the quadratic and cubic profiles are always more accurate, even for this small value of n. Results for the linear profile have not been included, since they are again generally worse than the CIM unless $n \gg 4$. Wood [23, 40] considers the linear profile applied to this problem and, as for the Bell and Abbas solution described in section 2.2, a three-term recurrence relation can be found, leading to a nonlinear polynomial equation to be solved for the unknown temperature coefficients. However, we have found that using either quadratic or cubic profiles gives much more accurate results.

4.2. The Time-Dependent Problem

For time-dependent $h(t)$ in (56) we solve the resulting ODE system, which combines (53), with $\delta = s$, the Stefan condition (42), but with δ replaced by s, and the derivatives of the expressions (39), (40), and (63). The initial conditions for the coefficients come from the classic Stefan problem, provided that $h(0) = 1$, in addition to $s(0) = 0$. The solution is tested for the case of an oscillating temperature prescribed at the surface boundary. Following Sadoun et al. [35], we set $h(t) = 1 - \epsilon \sin(\omega t)$, where ε and ω are the oscillation amplitude and frequency, respectively.

Results are given in Figure 4 with $\varepsilon = 0.5$ and $\omega = \pi/2$. The numerical solution shown is the second-order-accurate Keller box finite-difference scheme [22]. Since the temperature profile can have a peak developing for certain times, we only plot the cubic profile (with $n = 4$), as this performed significantly better for the time-dependent thermal problem (as shown the bottom right plot in Figure 2). We compare our solution to those from [35], which is the polynomial RIM profile (65) with $m = 2$. This is an example where the CIM polynomial breaks down; m quickly becomes less than unity as t increases (occurring when $t = 0.316$ for this example). Sadoun et al. do not show plots for the temperature profiles, and so their results are misleading: They

Table 1. Results for the classic Stefan problem (54)–(57) with $h(t) = 1$. The quadratic and cubic profiles use $n = 4$

	Percent error in α			Maximum error for T at $t = 1$		
β	Quadratic	Cubic	CIM	Quadratic	Cubic	CIM
0.1	2.35×10^{-1}	2.42×10^{-2}	2.161	4.61×10^{-3}	2.08×10^{-4}	2.28×10^{-2}
1	1.46×10^{-1}	1.05×10^{-3}	2.52×10^{-1}	1.32×10^{-3}	1.25×10^{-5}	9.22×10^{-3}
10	2.44×10^{-2}	2.887×10^{-5}	4.39×10^{-3}	2.40×10^{-4}	2.80×10^{-7}	1.41×10^{-3}

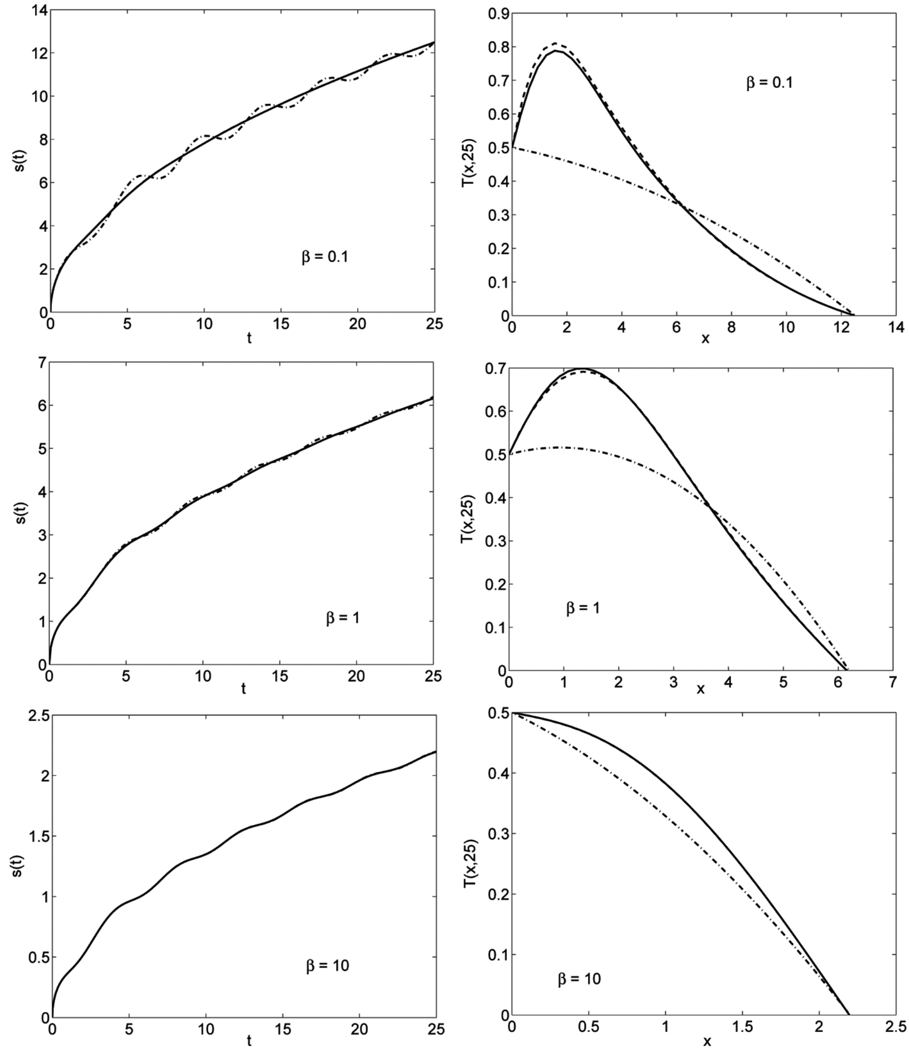

Figure 4. Plots of s of t and T against x (at $t = 25$) for various values of 3. The solid line is a numerical solution [22], the dashed line is the cubic profile (with $n = 4$), and the dot-dashed line is Sadoun's solution [35].

conclude that their RIM solution performs well for large β, but our results show that this is only true for s and not for T. The cubic profile, with $n = 4$, gives very accurate results for s for a large range of values of β. The top right plot in Figure 4 shows that we would need to use a larger value of n to correctly capture the temperature profile for small β, but still a value of $n < 10$ would be sufficient. The RIM solution completely fails to capture the peak in this case. In fact, results are not given in [35] for $\beta = 0.1$, which is where the single polynomial profile performs the worst. This is supported by an asymptotic analysis in [27], where, for the classic Stefan problem, the single HBIM profile does not give the correct limiting behavior for s as $\beta \to 0$, whereas it does as $\beta \to \infty$.

5. CONCLUSIONS

The aim of this work was to develop a general framework to accurately approximate the solution to one-dimensional heat transfer problems, both with and without a change of phase, using the nodal heat balance integral method. Although this technique is well documented, all previous analysis has focused on standard test problems which have exact solutions. In addition, most work uses piecewise linear profiles and therefore requires a large number of subdivisions to accurately capture the solution. There have been some studies using higher-order profiles, for example, quadratic profiles in [2, 3] and up to seventh-order polynomials in [40], but again these are applied only to standard test problems. It is mainly for other boundary conditions, such as the time-dependent conditions considered here, that linear profiles break down (as shown in the bottom right plot in Figure 2). The boundary immobilization technique removes the need to introduce a special starting procedure at $t = 0$, and naturally shows the correct initial conditions to use, by examining the limit of the transformed equations as $t \to 0$.

We conclude that using a cubic profile with a small number of subdivisions gives very accurate results for all the examples shown, and also ensures a smooth profile for the derivative. Although we could follow [40] and use more terms in the polynomial expansion, a cubic profile seems sufficient to accurately predict the correct solution, even when the boundary condition is a monotonically decreasing time-dependent function or an oscillatory function. Goodman [11] himself noted that the classic heat balance integral method is useful only for time-dependent boundary conditions that are monotonically increasing or constant. We argue that using higher-order polynomials would detract from the simplicity that has made the heat balance integral method so popular.

Another nice feature is that introducing the heat penetration depth δ into the numerical approach gives a natural way to convert a semi-infinite domain into a finite domain. Other numerical methods have to choose an arbitrary finite value for this boundary, which could lead to significant errors if it is not large enough, or be computationally expensive if it is overestimated to try and reduce these errors. This has been highlighted here for the simple thermal problem without a change of phase but could easily extended to problems where phase change does occur on a semi-infinite domain, such as ablation-type Stefan problems [18] and two-phase semi-infinite Stefan problems [20, 27].

APPENDIX A: THE LOGARITHMIC PROFILE

As mentioned in Section 2, an alternative to the polynomial profile (6) was developed by Mitchell and Myers [21]. There they proposed a profile of the form

$$T = \left(1 - \frac{x}{\delta}\right)^m \left[1 + \phi \ln\left(1 - \frac{x}{\delta}\right)\right] \tag{66}$$

The motivation for using this profile came from examining the thermal problem (1, 2, 4) but with the boundary condition (3) replaced by the time-dependent condition $T(0, t) = h(t)$. The most commonly used standard polynomial profile (6) cannot represent certain forms of $h(t)$, namely, monotonically decreasing conditions like

$h(t) = 1 - t$, since it permits a turning point only at $x = \delta$. After a certain time the exact solution has the internal temperature being greater than at this left boundary. The logarithmic profile (66) does satisfy the requirements $T_x = 0$ at both $x = \delta$ and $x = p$, where $0 < p < \delta$. Also, the condition (7) is automatically satisfied provided $m > 2$.

Following a similar argument to that in (7), we use the boundary condition $T(0, t) = h(t)$ to deduce

$$h_t = \frac{\partial T}{\partial t}(0, t) = \frac{\partial^2 T}{\partial x^2}(0, t) \tag{67}$$

Substituting (66) into (67) then leads to the expression

$$\phi = \frac{h_t \delta^2 - m(m-1)h}{2m - 1} \tag{68}$$

Note that the standard form for the temperature, Eq. (6), is retrieved by setting $\phi = 0$ in (66). As with the standard profile, (6), this profile now involves only two unknowns, m and δ. For a general $h(t)$, and without assuming m constant, substituting for the temperature profile (66) in the HBIM and RIM equations (8, 9) leads to

$$\text{HBIM: } \frac{d}{dt}\left[\frac{h\delta}{m+1} - \frac{\delta\phi}{(m+1)^2}\right] = \frac{mh + \phi}{\delta} \tag{69}$$

$$\text{RIM: } \frac{d}{dt}\left[\frac{h\delta^2}{(m+1)(m+2)} - \frac{(2m+3)\delta^2\phi}{(m+1)^2(m+2)^2}\right] = h \tag{70}$$

These are the two equations that now define the problem for a time-dependent boundary condition. With $\phi = 0$, $h = 1$, we retrieve the equations in (10). Then the CIM involves solving these two equations simultaneously, whereas for the minimization method we solve either (69) or (70) and choose m from minimizing $E = \int_0^\delta (T_t - T_{xx})^2 \, dx$.

APPENDIX B: THE QUADRATIC PROFILE

Here we give details of the method described in Section 3 using the quadratic profile, for boundary condition (i). This involves setting $\gamma_i = 0$ in (38), (39), and the first equation in (40) (the second equation is not required). Expressions for α_{n-1} and β_{n-1} are now given by $\alpha_{n-1} = -2F_{n-1}$ and $\beta_{n-1} = F_{n-1}$, and so instead of (43) and (44) we have

$$\delta\delta_t = \frac{6n^2}{3n - 2} \tag{71}$$

and

$$\alpha_i + 2(1-n)\beta_i - 2(i+1)(F_{i+1} - F_i) = 0 \quad i = 0, 1, \ldots, n-2 \tag{72}$$

It should be noted that an alternative approach considered by Bell [3, 4], and discussed in the Introduction, is to subdivide the dependent variable F_i into n equal intervals and then solve for the ξ_i's instead of the F_i's. An identical profile to (38) could still be used, but instead of (42), the heat balance integral would be

$$\delta\delta_t\left[\frac{\xi_{i+1}}{n}+(\xi_{i+1}-\xi_i)\left(\frac{\alpha_i}{2}+\frac{\beta_i}{3}+\frac{\gamma_i}{4}\right)\right]=\frac{2\beta_i+3\gamma_i}{\xi_{i+1}-\xi_i} \tag{73}$$

and instead of (40), matching first and second derivatives gives

$$\frac{\alpha_i+2\beta_i+3\gamma_i}{\xi_{i+1}-\xi_i}=\frac{\alpha_{i+1}}{\xi_{i+2}-\xi_{i+1}} \quad \frac{2(\beta_i+6\gamma_i)}{\xi_{i+1}-\xi_i}=\frac{2\beta_{i+1}}{\xi_{i+2}-\xi_{i+1}} \tag{74}$$

In this case, setting $i=n$ in (73) does not give an explicit expression for $\delta\delta_t$ only in terms of n; here the unknown ξ_n is present. We would therefore have a system of nonlinear equations to solve for the unknown coefficients and λ, assuming $\delta=2\lambda\sqrt{t}$. Subdividing the spatial variable ξ gives a much simpler formulation, and so we do not consider this alternative approach further. It also more naturally corresponds to other numerical methods, such as finite-difference methods, where the independent variable is also subdivided equally [22].

REFERENCES

1. J. A. Addison, S. D. Howison, and J. R. King, Ray Methods for Free Boundary Problems, *Quart. Appl. Math.*, vol. LXIV, no. 1, pp. 41–59, 2006.
2. G. E. Bell, Solidification of a Liquid about a Cylindrical Pipe, *Int. J. Heat Mass Transfer*, vol. 22, pp. 1681–1686, 1979.
3. G. E. Bell, A Refinement of the Heat Balance Integral Method Applied to a Melting Problem, *Int. J. Heat Mass Transfer*, vol. 21, pp. 1357–1362, 1978.
4. G. E. Bell and S. K. Abbas, Convergence Properties of the Heat Balance Integral Method, *Numer. Heat Transfer*, vol. 8, pp. 373–382, 1985.
5. W. F. Braga, M. B. H. Mantelli, and J. L. F. Azevedo, Analytical Solution for One-Dimensional Semi-Infinite Heat Transfer Problem with Convection Boundary Condition, *AIAA Thermophys. Conf.*, June 2005.
6. T. W. Brakel, J. P. F. Charpin, and T. G. Myers, One Dimensional Ice Growth due to Incoming Supercooled Droplets Impacting on a Thin Conducting Substrate, *Int. J. Heat Mass Transfer*, vol. 50, pp. 2694–2705, 2007.
7. J. Caldwell and C. K. Chiu, Numerical Solution of One-Phase Stefan Problems by the Heat Balance Integral Method, Part I: Cylindrical and Spherical Geometries, *Commun. Numer. Meth. Eng.*, vol. 16, pp. 569–583, 2000.
8. J. Caldwell and Y. Y. Kwan, Starting Solutions for the Boundary Immobilization Method, *Commun. Numer. Meth. Eng.*, vol. 21, pp. 289–295, 2005.
9. J. Caldwell and Y. Y. Kwan, Numerical Methods for One-Dimensional Stefan Problems, *Commun. Numer. Meth. Eng.*, vol. 20, pp. 535–545, 2004.
10. J. Caldwell and S. Savović, Numerical Solution of Stefan Problem by Variable Space Grid and Boundary Immobilization Method, *J. Math. Sci.*, vol. 13, pp. 67–79, 2002.
11. T. R. Goodman, The Heat-Balance Integral and Its Application to Problems Involving a Change of Phase, *Transfer ASME*, vol. 80, pp. 335–342, 1958.

12. T. R. Goodman, Application of Integral Methods to Transient Nonlinear Heat Transfer, *Adv. Heat Transfer*, vol. 1, pp. 51–122, 1964.
13. T. R. Goodman and J. J. Shea, The Melting of Finite Slabs, *J. Appl. Mech.*, vol. 27, pp. 16–27, 1960.
14. J. M. Hill, *One-Dimensional Stefan Prolems: An Introduction*, Longman, Harlow, UK, 1987.
15. J. Hristov, The Heat-Balance Integral Method by a Parabolic Profile with Unspecified Exponent: Analysis and Exercises, *Thermal Sci.*, vol. 13, no. 2, pp. 27–48, 2009.
16. S. Kutluay, A. R. Bahadir, and A. Ozdes, The Numerical Solution of One-Phase Classical Stefan Problem, *J. Comput. Appl. Math.*, vol. 81, pp. 134–144, 1997.
17. D. Langford, The Heat Balance Integral Method, *Int. J. Heat Mass Transfer*, vol. 16, pp. 2424–2428, 1973.
18. S. L. Mitchell and T. G. Myers, A Heat Balance Integral Method for One-Dimensional Finite Ablation, *AIAA J. Thermophys.*, vol. 22, no. 2, pp. 508–514, 2008.
19. S. L. Mitchell and T. G. Myers, Approximate Solution Methods for One-Dimensional Solidification from an Incoming Fluid, *J. Thermophysics Heat Transfer*, vol. 202, no. 1, pp. 311–326, 2008.
20. S. L. Mitchell and T. G. Myers, Application of Standard and Refined Heat Balance Integral Methods to One-Dimensional Stefan Problems, *SIAM Rev.*, vol. 52, no. 1, pp. 57–86, 2010.
21. S. L. Mitchell and T. G. Myers, Improving the Accuracy of Heat Balance Integral Methods Applied to Thermal Problems with Time Dependent Boundary Conditions, *Int. J. Heat Mass Transfer*, vol. 53, pp. 3540–3551, 2010.
22. S. L. Mitchell and M. Vynnycky, Finite-Difference Methods with Increased Accuracy and Correct Initialization for One-Dimensional Stefan Problems, *Appl. Math. Comput.*, vol. 215, pp. 1609–1621, 2009.
23. F. Mosally, A. S. Wood, and A. Al-Fhaid, On the Convergence of the Heat Balance Integral Method, *Appl. Math. Comput.*, vol. 29, pp. 903–912, 2005.
24. T. G. Myers, Optimizing the Exponent in the Heat Balance and Refined Integral Methods, *Int. Commun. Heat Mass Transfer*, vol. 36, pp. 143–147, 2009.
25. T. G. Myers, An Approximate Solution Method for Boundary Layer Flow of a Power Law Fluid over a Flat Plate, *Int. J. Heat Mass Transfer*, vol. 53, pp. 2337–2346, 2010.
26. T. G. Myers, Optimal Exponent Heat Balance and Refined Integral Methods Applied to Stefan Problems, *Int. J. Heat Mass Transfer*, vol. 53, pp. 1119–1127, 2010.
27. T. G. Myers and S. L. Mitchell, Application of the Combined Integral Method to Stefan Problems, *Appl. Math. Model.*, vol. 35, pp. 4281–4294, 2011.
28. S. L. Mitchell and T. G. Myers, *Measuring the Error for Heat Balance Integral Methods*, Submitted, 2011, March.
29. T. G. Myers and S. L. Mitchell, Application of the Heat Balance and Refined Integral Methods to the Korteweg-de Vries equation, *Thermal Sci.*, vol. 13, no. 2, pp. 113–119, 2009.
30. T. G. Myers, S. L. Mitchell, G. Muchatibaya, and M. Y. Myers, A Cubic Heat Balance Integral Method for One-Dimensional Melting of a Finite Thickness Layer, *Int. J. Heat Mass Transfer*, vol. 50, pp. 5305–5317, 2007.
31. B. Noble, Heat balance methods in melting problems, in J. R. Ockendon and W. R. Hodgkins (eds.), *Moving Boundary Problems in Heat Flow and Diffusion*, pp. 208–209, Clarendon Press, Oxford, 1974.
32. V. Novozhilov, Application of Heat-Balance Integral Method To Conjugate Thermal Explosion, *Thermal Sci.*, vol. 13, no. 2, pp. 73–80, 2009.
33. K. Pohlhausen, Zur naherungsweisen Integration der Differentialgleichunger der laminaren Grenzschicht, *Z. Math. Mech.*, vol. 1, pp. 252–258, 1921.

34. G. Poots, On the Application of Integral Methods to the Solution of Problems Involving the Solidification of Liquids Initially at Fusion Temperature, *Int. J. Heat Mass Transfer*, vol. 5, pp. 525–531, 1962.
35. N. Sadoun, E.-K. Si-Ahmed, and P. Colinet, On the Refined Integral Method for the One-Phase Stefan Problem with Time-Dependent Boundary Conditions, *Appl. Math. Modell.*, vol. 30, pp. 531–544, 2006.
36. N. Sadoun, E.-K. Si-Ahmed, P. Colinet, and J. Legrand, On the Goodman Heat-Balance Integral Method for Stefan Like Problems: Further Considerations and Refinements, *Thermal Sci.*, vol. 13, pp. 81–96, 2009.
37. S. K. Sahu, P. K. Das, and S. Bhattacharyya, How Good Is Goodman's Heat-Balance Integral Method for Analyzing the Rewetting of Hot Surfaces?, *Thermal Sci.*, vol. 13, no. 2, pp. 97–112, 2009.
38. S. Savović and J. Caldwell, Finite-Difference Solution of one-Dimensional Stefan Problem with Periodic Boundary Conditions, *Int. J. Heat Mass Transfer*, vol. 46, pp. 2911–2916, 2003.
39. H. Schlichting, *Boundary layer theory*, 8th ed., Springer, Verlag, Berlin, 2000.
40. A. S. Wood, F. Mosally, and A. Al-Fhaid, On Higher-Order Polynomial Heat-Balance Integral Implementations, *Thermal Sci.*, vol. 13, no. 2, pp. 11–25, 2009.
41. A. S. Wood, A New Look at the Heat Balance Integral Method, *Appl. Math. Modell.*, vol. 25, no. 10, pp. 815–824, 2001.